

US7-VALIDATION OF MATERIAL MODELS: NON-DESTRUCTIVE TESTING THROUGHOUT THE DEVELOPMENT OF A CARBON-FIBER COMPOSITE AUTOMOTIVE CRASH STRUCTURE

*Cameron J. Dasch
Highwood Technology LLC*

*Martin H. Jones
Ford Motor Company*

Abstract

Throughout the development of the recent USCAR carbon-fiber composite front-bumper/crush-can (FB-CC) structure, non-destructive evaluations (NDE) were used to verify the quality of the materials, joining, and assembly. NDE was used at each stage in the program, from flat plaques to simple box-sections to final 3-D structure, and included both as-built and crashed components. Discrepancies of concern included voids, delaminations, foreign materials, fabrication errors and damage. The methods selected were chosen for sensitivity, speed, and ability to deal with complex 3-D structures. These methods included ultrasonic pulse/echo (both conventional and phased-array), low-energy x-ray radiography, computed tomography (CT), and optical surface scans. This is a case study of how NDE can accelerate the carbon-composite component development process and how to modify a component to facilitate NDE. Innovations included molded-in inserts to test defect detectability, compression-after-impact to establish minimum resolution, adhesive verification, ultrasonic measurement of ply-orientations, and the use of 3-D printed parts to test NDE procedures before final parts were available.

Background and Requirements

As the need for improved fuel-economy in automotive vehicles increases, the replacement of denser materials with carbon composites will inevitably increase. Since the earliest days of carbon composites, nondestructive testing has been used to verify the fabrication. This is primarily a result of the processing of these composites which start with fibers, matrix and embedded air, pass through a semi-fluid state under pressure and heat, and finally undergo solidification. A host of different methods have been used to detect the many possible discrepancies that can be introduced during the manufacture of these composites. These discrepancies include porosity, lack of fiber wetting, cracks including delamination, foreign matter contamination, lack of cure, missing and mis-oriented plies, and part distortion to name a few.^{1,2} Under good processing controls, many of these such as fiber wetting and curing are not usually an issue.

Automotive applications of carbon composites have come relatively recently but have some significant differences from the much more wide-spread aeronautical and wind-turbine applications. The components will be relatively small, thin, highly 3-dimensional, and very cost sensitive. Automotive structural components are likely to be safety critical and must be able to withstand many impacts over their lifetime, such as stone-hits and parking lot impacts. These will almost always lead to the use of woven, quasi-isotropic layups which have very good impact resistance and a low propensity to delaminate.

The objective of this four-year U.S. DOE and USAMP Cooperative Agreement project is to validate and assess the ability of physics-based material models to predict crash performance of primary load-carrying carbon fiber composite automotive structures. Predictions are being compared to experimental results from quasi-static testing and dynamic crash testing of a lightweight carbon fiber composite front bumper (FB) and crush can (CC) system which was selected for demonstration via design, analysis, fabrication, and crash testing. The successful validation of these crash models will facilitate improved design of lightweight carbon fiber composites in automotive structures for significant mass savings.

The nondestructive testing in this project has been driven by the need to support all phases of the material/processing development as well as destructive mechanical testing. This is shown schematically in Figure 1 by the three stages of the material development: from flat plaques, to a relatively simple hat-section part, and finally to the designed front bumper and crush can. The methods selected needed to handle the 3-Dimensional shapes, to be rapid, and to be readily available throughout the automotive manufacturing environment.

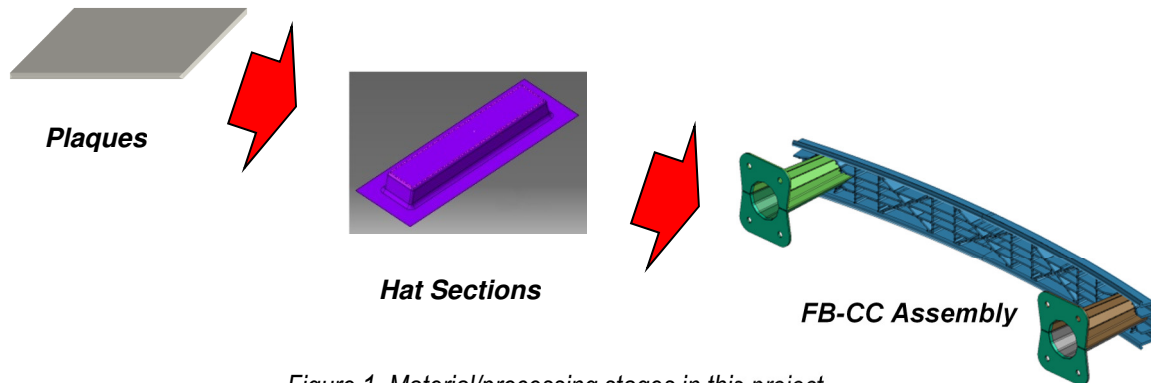


Figure 1. Material/processing stages in this project

The methods selected included low-energy x-ray radiography, x-ray computed tomography (CT), pulse/echo ultrasonics, and optical surface mapping. The performance of these methods on flat plaques, hat-sections, and bonded structures have been previously discussed.^{3,4}

The NDE methods selected are complimentary to each other. The x-ray and optical methods can easily handle the 3-Dimensionality of the parts, although low x-ray energies are necessary to maximize material contrast. To cover the entire FB-CC assembly, multiple regions are individually imaged and then must be spliced together. These methods have limited ability to detect delaminations. Ultrasonic pulse/echo can be very good for detecting delaminations, but is very sensitive to deviations of the focused beam from the surface normal. Only the flat sections of the crush cans and front bumper were ultrasonically imaged. To maximize the ultrasonic imaging, the crush cans were specifically designed to have flat facets and polyhedral shape rather than a cylindrical surface. Each of the facets is roughly 25-mm wide and could be imaged by a single pass of an ultrasonic phased array.

In order to determine the needed resolution and sensitivity, two important strategies were used. The first was to establish the needed spatial resolution by using compression-after-impact testing to determine the fall-off in strength as a function of impact energy and damage area.³ This approach has been used by others^{5,6} and works fairly well when the ASTM methods are modified for thin (<5 mm thick) composites. Typically, delaminations of <6mm have negligible effect on the strength of quasi-isotropic materials. The second strategy is to prepare test parts with thin polyethylene (PE) or polytetrafluoroethylene (PTFE) inserts to simulate delaminations. In this work, the inserts are placed at a variety of locations and all the inter-ply

to determine the sensitivity of the different NDE methods throughout the assembly.

Not untypically, there was a very tight time window between when the final design of the components was completed and when production parts would be made. To exercise the inspection methods on the final 3-D components, the two crush-can halves and part of the front-bumper were 3-D printed in nylon. This is a very useful approach to verify the inspection fixtures and orientation of the part relative to the NDE excitation source.

The following sections give the experimental details and illustrate the performance on the crush-can and front-bumper can components and on adhesively-bonded assemblies. The results for the crashed components will be detailed elsewhere.

Experimental

The FB-CC structure is assembled from five pieces: each crush can is riv-bonded from two half-sections while the bumper is a single ribbed piece (see Fig 1). The crush cans are adhesively bonded into pockets in the front bumper. There are three different materials in the bumper and crush-cans. The primary material is a 2x2 twill-woven carbon-fiber fabric pre-preg with an epoxy matrix. The flat surfaces of both the crush-can and front bumper used quasi-isotropic layups of this woven composite: the CC uses 12 plies (2.9-mm thick) while the FFB has 24 plies (5.8-mm thick). The rear mounting-flange of the crush-can is a glass-fiber SMC that infiltrates fabric tabs that blend into the rear flange. The ribs of the front-bumper are a carbon-fiber SMC.⁷

To determine the sensitivity of the detection methods, both a bumper and crush can were fabricated with thin (75- μm), 6-mm diameter PE and PTFE inserts. The inserts are placed at a variety of locations and all the inter-ply to determine the sensitivity of the different NDE methods throughout the assembly. This size discrepancy was determined from compression-after-impact testing of the primary fabric composite.

The x-ray radiography used a source with a beryllium window and performed well at very low energies (20-35 keV). The imaging plate gave a field of view of about 300-mm but the facility could accommodate the entire assembly. At the lowest energies, the adhesive could be resolved from the composite and was used to ensure adequate adhesive spread. The PTFE inserts could be detected but not the PE inserts. At these energies there is also very high contrast between the woven materials and the glass-fiber SMC.

The computed tomography used somewhat higher energy x-rays (50-110 keV) to get adequate penetration through all chords of the assembly including the rivets. The CT volume was roughly 250-mm on a side with a resolution of 0.1-mm per voxel. This CT volume-resolution tradeoff was chosen to give adequate resolution to detect porosity while requiring only five scans to image the entire FB-CC assembly. The CT scanner could not accommodate the entire assembly, and it was necessary to cut the assembly into five pieces. A typical CC section is shown in Fig. 2c. At this resolution and these energies, the individual plies and the adhesive are not individually resolved.

Ultrasonic pulse/echo imaging was performed in an immersion bath with a linear phased array. The array was mounted in a small surface-riding fixture and manually translated along the surface aligned by a guide bar. The position along the guide bar is determined with a string encoder. Each scan covers an area 25-mm wide and the length of the crush can or bumper. These scan-strips are patched together to give an image of the entire surface. The ultrasonic array was designed specifically for the inspection of thin automotive materials (1-3mm thick). The elements have a center frequency of 17-MHz and a wide bandwidth (>70%) to give good

depth resolution. There are 64- elements with an element pitch (spacing) of 0.4-mm and element height of 4-mm. The array surface is contoured to give a transverse cylindrical focus. Typically 10-elements are grouped to give a final roughly 4-mm diameter, 25-mm focal length beam. The speed of sound in these materials (50% volume fraction carbon fiber in epoxy) is 3.0 mm/ μ sec. While this array is very useful on thin aluminum and steel materials, the frequency is higher than the optimum for carbon composites with a polymeric matrix due to the severe beam attenuation. For a 3-mm thick CFRP composite, the round-trip transmission is typically <10%. A better compromise with adequate depth resolution (<0.06 mm), would be 12-MHz which typically has a round-trip transmission of 30%.

To exercise the inspection methods on the final 3-D design but prior to making composite parts, the two crush can components and part of the front-bumper were printed in nylon using a stereo lithography (SLS) process. This section is shown in Fig. 2 along with the CAD design and the final composite section.

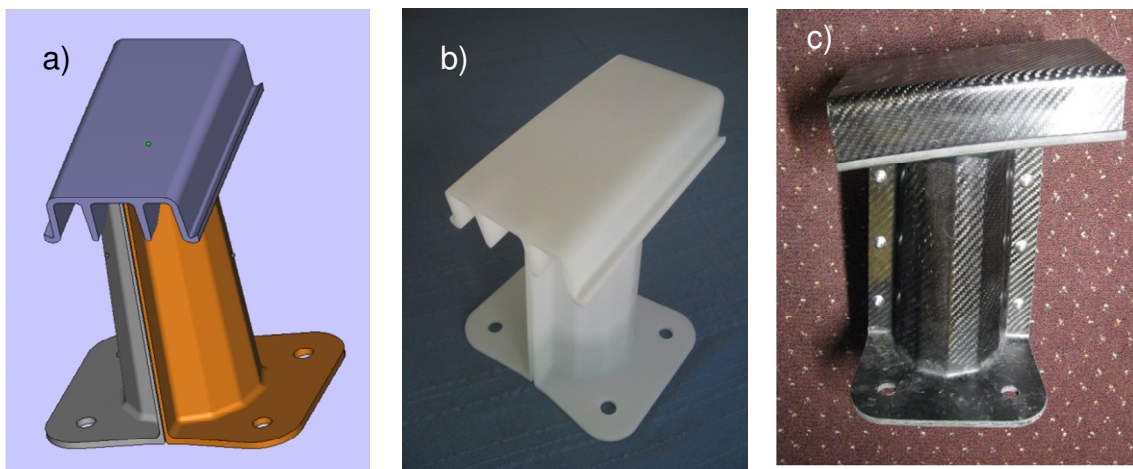


Figure 2. Three versions of the FB-CC joint used in this project, a) CAD design, b) SLS 3-D nylon prototype, and c) carbon-composite section used in a CT scan.

Results

Detection Sensitivity Using Thin Inserts

From the earlier compression-after-impact tests³, it was determined that discrepancies 6-mm in size or smaller would have negligible effect on the strength of the woven CRFP composite. Both PE and PTFE inserts were fabricated into a CC and a FB. Several inserts were placed on each layer as the plies were stacked. Figures 3 and 4 show the intended locations of the inserts as well as the radiographic and ultrasonic images obtained. The positioning of the inserts was not very accurate. In the crush cans, radiography was able to detect the PTFE inserts which had a significantly higher density. However, as seen in the earlier round work the PE inserts cannot be discerned, even at x-ray energies as low as 20 keV. In the bumpers, only a few of the PTFE inserts can be seen when they lie away from the ribs.

Ultrasonic pulse/echo can detect most of the PTFE inserts and the shallower PE inserts. The discrimination with the phased array had reduced performance compared to single-element transducers of comparable aperture. These C-scans are raw peak internal echoes without time-

distance amplitude corrections which would improve the detection. The ultrasonic performance on the front bumpers was similar.

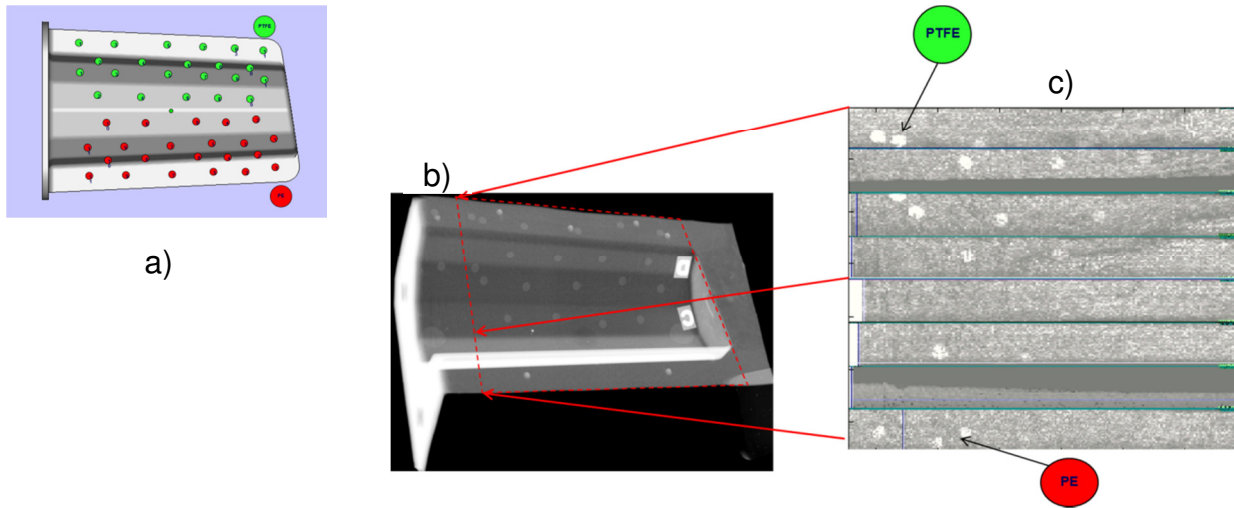


Figure 3. Detection sensitivity on a crush-can half-section using thin PE and PTFE inserts. a) Schematic of insert locations, b) low-energy radiograph showing PTFE inserts, and c) high-frequency ultrasonic C-scan of PE and PTFE inserts.

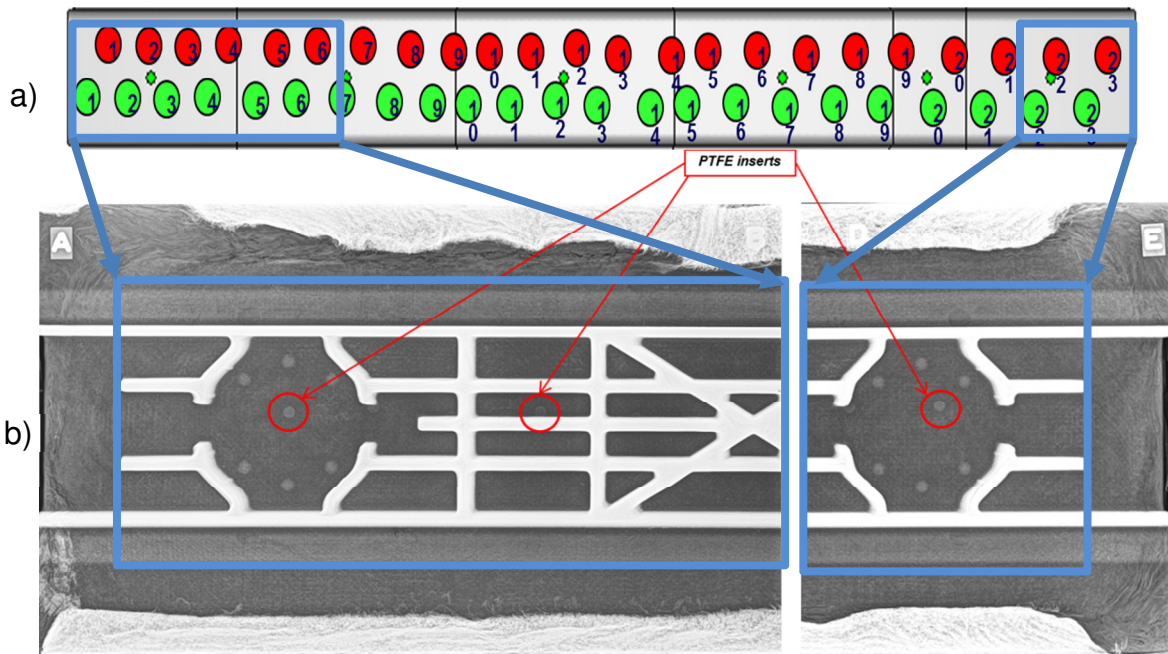


Figure 4. Detection sensitivity on a front bumper using thin PE and PTFE inserts. a) Schematic of insert locations and b) low-energy radiograph showing PTFE inserts.

Crush Can Features

The results of inspecting the crush can halves are shown in Figures 5-8. The optical surface scans provide maps of both the thickness and deviations from the CAD model (Fig 5). The surfaces were typically within 0.1-mm of the thickness specification and the surfaces were on average within 0.3-mm of the CAD surface. Some parts such as shown in Fig. 5 show a small amount of part distortion at a maximum of 0.5-mm. This was acceptable for the assembly of the components.

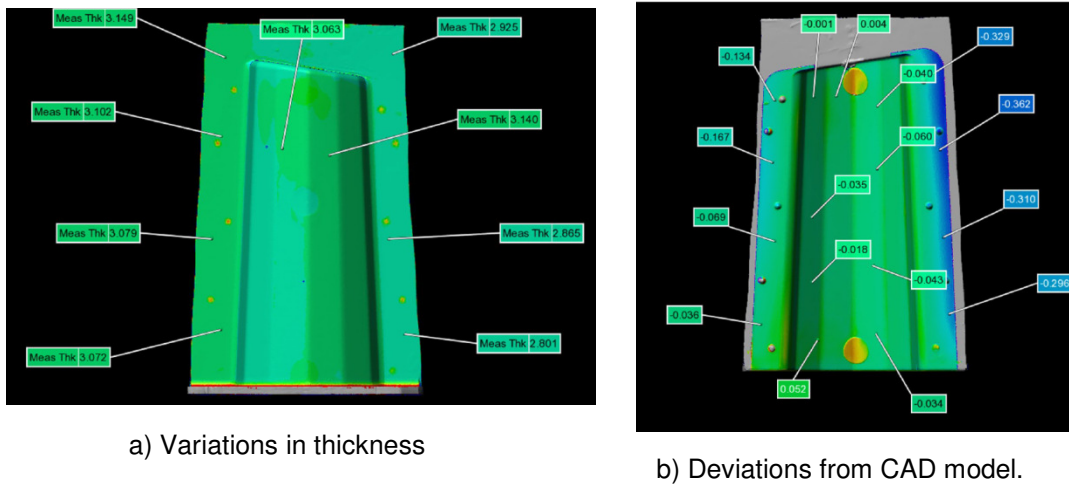


Figure 5. Optical surface mapping. a) Variations in surface thickness, b) deviations of the outer surface from the CAD model.

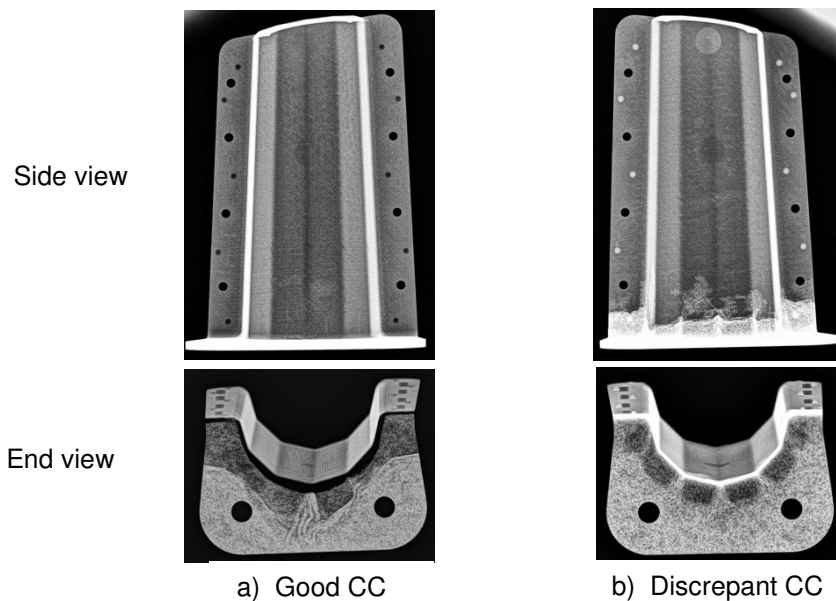


Figure 6. Low-energy radiographs (side view and end view) of crush can. The end views show the fabric tab pattern variation due to SMC flow. a) "Good" CC with low dart location and low intrusion of SMC and b) Discrepant CC with high dart location and higher intrusion of SMC.

Low energy radiographs were especially useful in this project (see Fig. 6). Typically two views were taken: a side-view of the facets and side-flanges and an end-view of the rear flange. The glass-fiber SMC in the rear flange has much higher attenuation than the fabric CFRP in the sides. The side views detected that some CC's had discrepant movement of the SMC from the rear flange up along the facets (Fig. 6b). This would tend to squeeze resin from the pre-preg. This movement also may be associated with the stretch and bunching visually and ultrasonically observed in this rear region of the crush can. The end views show how the fabric is darted in order to create tabs that extend out into the rear flange. In the discrepant CC, it appears that the fabric has moved forward so the darts are above the rear flange radius. Even in the good CC, there appears to be movement in the fabric so that the tabs are less well defined.

Ultrasonic pulse/echo images using the phased array did not indicate any delaminations or foreign matter (see Fig. 7). The images from the facets as well as the side flanges are combined to create an unfolded image of the fabric area. Two scans of each area were taken to assure that all features were repeatable. Due to the array fixture size and non-imaging edge of the array, roughly 20-mm of each end of the facets could not be imaged. Also, the narrower facets next to the side flanges were not completely imaged. The indents used to align the two CC-halves are visible on the side-flanges. The only significant discrepancies observed are the vertical (circumferential) striations seen in Fig. 7c closer to the rear flange. Mechanical property testing found the discrepant CC (Fig. 7c) had significantly lower strength. The striations may be associated with folding or bunching of the fabric.⁷

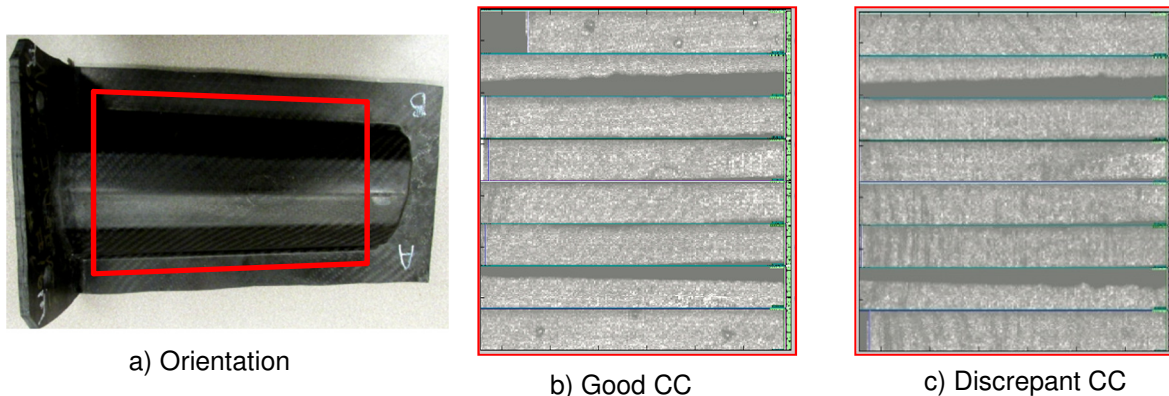


Figure 7. Ultrasonic pulse/echo C-scan of the CC side facets. The images from the facets and side flanges are collaged to into fold-out view. a) photo showing CC orientation, b) higher strength CC, and c) CC with reduced strength showing striations may come from fabric folding or bunching.

An example of the CT scans of two crush can section bonded together are shown in Fig. 8. The CT scans have a voxel size of 0.1-mm which is not adequate to resolve the individual plies of the fabric composite (Fig. 8). No porosity was observed within the fabric CFRP of the facets or side flanges. There was minor porosity in the adhesive.

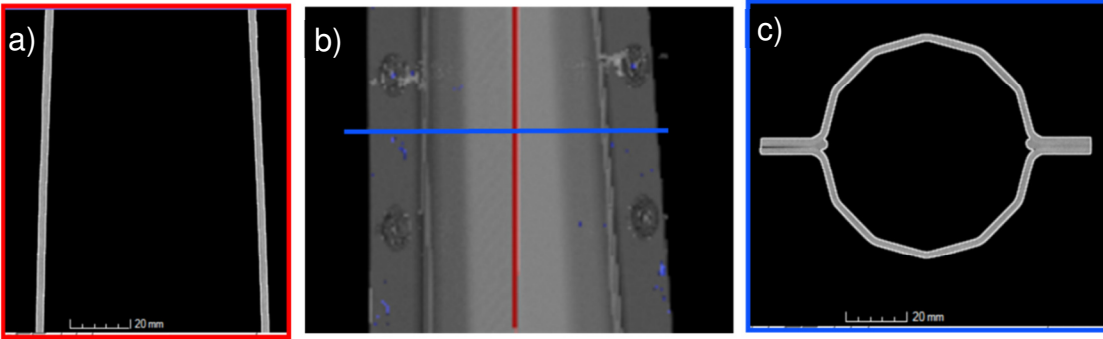


Figure 8. CT inspection of bonded crush can sections. a) vertical cut, b) perspective surface view showing location of cross-sections, c) cross-cut.

Front Bumper Inspection

The optical scan of the front bumper also showed that the thicknesses which were within specification. The bumper does present some technical problems since it is long and thin. Multiple sectional scans of the front, back and edges must be carefully pieced together using alignment targets. A map of the deviation of the surface of an as-molded, untrimmed bumper from the CAD model is shown in Fig. 9. The gray areas are outside the trim line. The maximum deviation was 1.6-mm over the 1000-mm length of the bumper. This was deemed acceptable and presented no assembly problems.

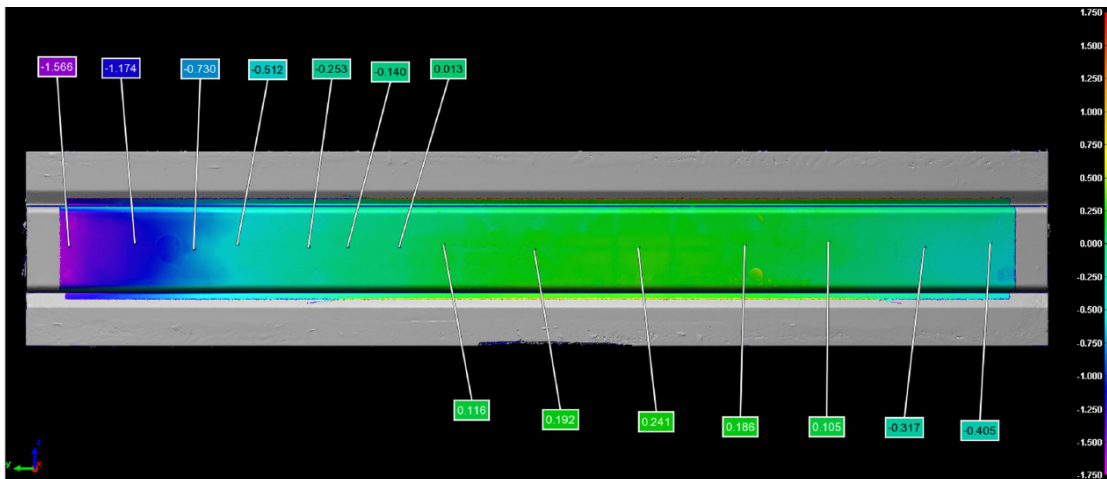


Figure 9. Optical surface map of an untrimmed front bumper showing deviations of the front surface from the CAD model. The gray areas are outside the trim line.

CT imaging was found to be the most useful tool for the complicated structure of the front bumper. This revealed porosity throughout the bumper ribs that are carbon-fiber SMC (See Fig. 10). Figure 10 is a superposition of the part density with a porosity analysis. The porosity surfaces are color coded to indicate the volume of each pore/crack. Sectioning of the bumper allowed a direct comparison of the CT to the polished micrograph. This is shown in the companion paper on the material processing.⁷

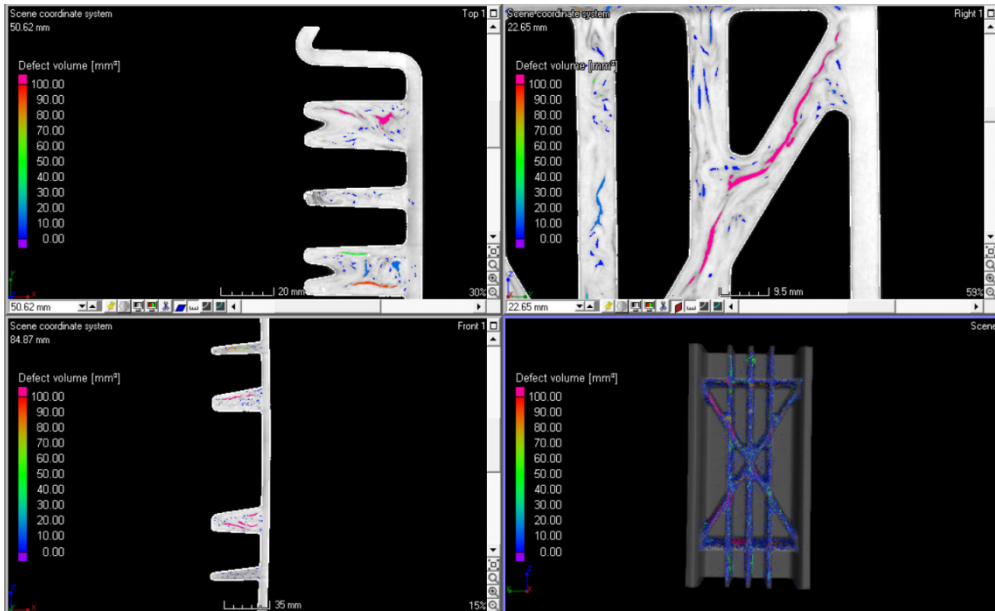
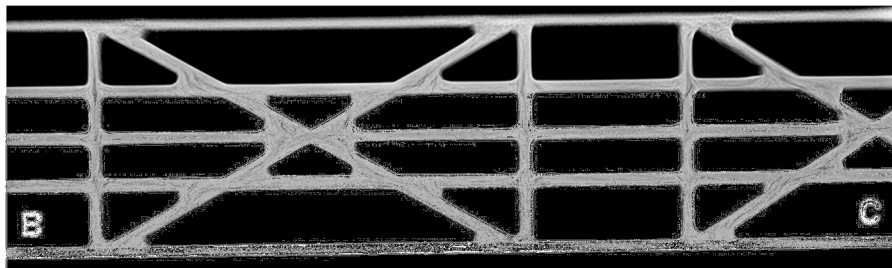
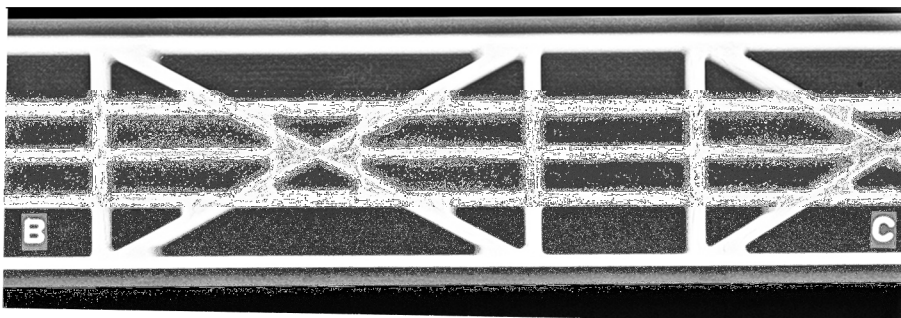


Figure 10. CT of FB section showing perspective view (lower right) and three orthogonal slices. These are composite images of the density (in gray) overlaid by a porosity analysis. The color of the porosity indicates the volume of the pore/crack.



a) Higher energy



b) Lower energy

Figure 11. Low-energy radiographs of a 250-mm long section of front bumper: a) Higher energy x-rays showing porosity and cracks in the SMC ribs and b) lower energy x-rays used to inspect front fabric surface for foreign matter.

Low energy radiography was primarily intended to detect foreign matter within the FB. This application is shown in Figure 11b with lower energy x-rays (about 35 keV). At these energies small variations in the FB woven material can be observed, but the ribs are strongly attenuating. At higher energies, with less attenuation by the ribs, the porosity/cracks seen in the CT scan can also be seen (Fig. 11a). This very fast diagnostic would be a useful tool for 100% inspection of a production bumper with ribs.

Assembly and Adhesive Joints Inspection

In the final assembly two CC sections are riv-bonded together into a CC sub-assembly which is then bonded into a molded socket in the front bumper. Details of the bonding are shown in Fig. 12 and 13. The entire assembly could be radiographic imaged in five sections with high contrast and resolution. The adhesive which is roughly 1-mm thick can be readily seen especially in the FB-CC interface. In the joint, an excess of adhesive is used to ensure complete coverage of the large interface. The bonding between the CC-halves is less evident because the side-flange area is completely filled. Early work showed that incomplete fill could be readily detected.³

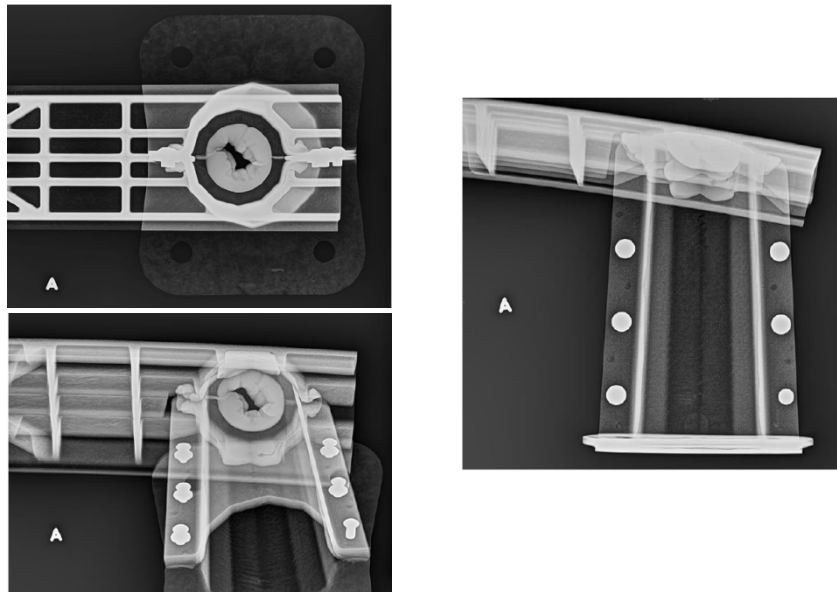


Figure 12. Radiographs of FB-CC assembly. There are three views of the same assembly. a) end view, b) side view, and off-axis view. The spread of the adhesive between the FB and CC can be seen. The adhesive completely fills the CC side flanges.

The assembly was too large to CT'ed as a single piece. It was necessary to cut the bumper into at least five pieces to fit into the medium resolution CT cabinet (See Fig. 13). All the FB sections exhibited the porosity discussed in Fig. 10. A small amount of porosity was seen in the CC side-flange joint, but most of this was associated with the alignment bumps/dimples on the surfaces or isolated air bubbles.

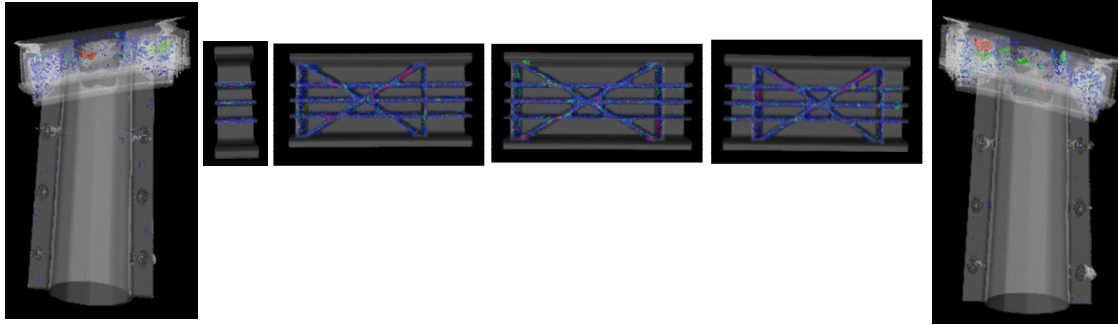


Figure 13. CT of FB-CC assembly. This is super position of the outer surface and a porosity analysis.

Summary and Next Steps

This work has shown automotive carbon composite components are amendable to nondestructive testing. This testing detected two major discrepancies that have a significant impact on the performance of the assembly. These were the movement of the fabric in the mold with the associated incursion of the SMC up the walls of the crush can and the porosity in the bumper's SMC ribs. These discrepancies were confirmed after the fact by sectioning and mechanical property testing. Both of the discrepancies involved the flow of the SMC around the fabric and were mostly elucidated by radiography and by tomography.

Ultrasonic pulse/echo proved to be less useful on the FBCC components than on the earlier flat plaque and top-hat sections. Ultrasonics can reveal a lot of the fabric structure under planar conditions. This includes very accurate fabric orientation measurements. However, in the FB-CC with a phased-array, the pulse-width is larger and the dynamic range is restricted. Furthermore, it was the SMC areas which were problematic. The most useful information from the ultrasonic imaging would have been to better quantify fabric folding, stretching, and bunching, rather than ply rotation.

Future work should focus on imaging transition areas such as the rear flange of the crush-can. These areas are inevitable in automotive components and can be areas of high stress. The issues associated with molding of SMC over fabric were not identified as a critical area until in the design and production phases of the project. Future programs should incorporate more destructive and mechanical property testing and should include 100% NDE testing of the components.

Acknowledgements

This work was supported by the US Department of Energy under Cooperative Agreement DE-EE0005661 awarded to the United States Automotive Materials Partnership. The views expressed are solely those of the authors. We are indebted to George Harmon of FCA for his invaluable role on this project and the elegant radiography. The CT scans were provided by Jesse Garant and Associates, Windsor, Ont. The authors would also like to gratefully acknowledge the project leaders Libby Berger and Omar Faruque, who assembled the USAMP Team as well as the team participants that provided the carbon-fiber components and insightful feedback on the NDE results.

Bibliography

1. "Carbon Composites and Cars – Technology Watch 2012", 2012. Reinf. Plast. 57(1): 39–42.
2. Heslehurst, R. B., 2014. Defects and Damage in Composite Materials and Structures, CRC Press.
3. Dasch, C. J., Harmon, G.J. and M. H. Jones, "Ultrasonic and X-ray Inspection of a High Performance Carbon Fiber Composite for Automotive Applications", Proceedings of the Meeting of the American Society for Composites, Lansing Michigan, Sept. 2015.
4. Dasch, C. J., J. A. Schroeder and D. L. Simon, "Non-Destructive Inspection of Adhesively Bonded Composites: Comparison of Thermal Wave Imaging, Ultrasonic and Radioscopy Methods", Proceedings of the Meeting of the American Society for Composites, Dearborn, MI, September 17-20, 2006.
5. Siow, Y. P. and V. P. W. Shim 1998. "An Experimental Study of Low Velocity Impact Damage in Woven Fiber Composites", J. Comp. Matls., 32: 1178-1198.
6. Yan, H., C Oskay, A. Krishnan, and L. Xu. 2010. "Compression-after-impact response of woven fiber-reinforced composites", Compos. Sci. Technol., 70: 2128–2136.
7. Coppola, A.M., L. Berger, G. Smith, D. Armstrong, and C.J. Dasch, "Validation of Material Models: Thermoset Composite Materials and Processing For a Composite Bumper Beam System", SPE ACCE, Sept. 2016, Novi MI.